Cell Stem Cell, Volume *26*

Supplemental Information

High-Efficiency, Selection-free Gene Repair in Airway Stem Cells from Cystic Fibrosis Patients Rescues CFTR Function in Differentiated Epithelia

Sriram Vaidyanathan, Ameen A. Salahudeen, Zachary M. Sellers, Dawn T. Bravo, Shannon S. Choi, Arpit Batish, Wei Le, Ron Baik, Sean de la O, Milan P. Kaushik, Noah Galper, Ciaran M. Lee, Christopher A. Teran, Jessica H. Yoo, Gang Bao, Eugene H. Chang, Zara M. Patel, Peter H. Hwang, Jeffrey J. Wine, Carlos E. Milla, Tushar J. Desai, Jayakar V. Nayak, Calvin J. Kuo, and Matthew H. Porteus

Figure S1

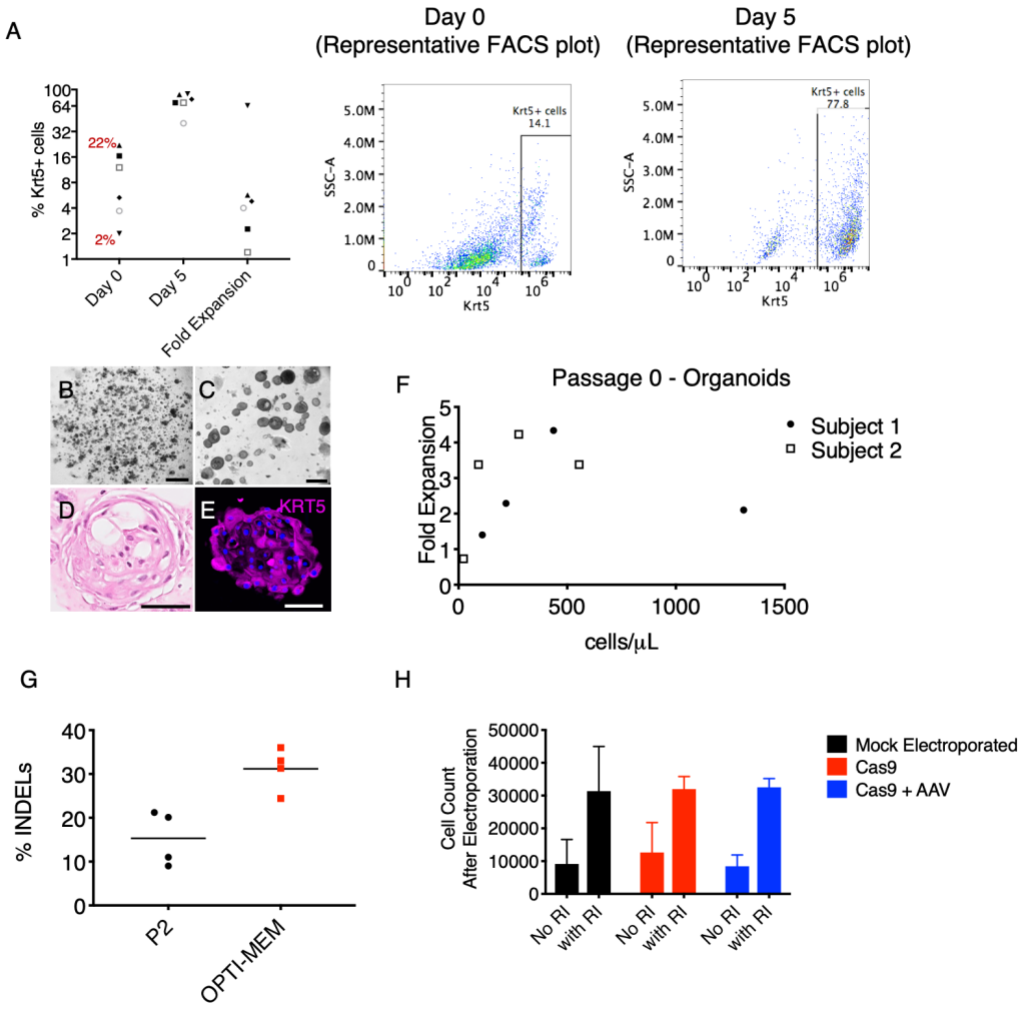

Figure S1. Characterization of human UABC organoids, Related to Figure 1 (A) Percent KRT5+ cells on day 0 (2 - 22%, average ± SD = 10 ± 8%), day 5 (40-90%, average ± SD = 72 ± 18%) and fold expansion observed in 6 subjects (2 - 64%). Representative FACS plots of UABC organoids with KRT5+ gating on day 0 versus day 5. **(B-E)** Primary human UABCs were cultured as organoids in BME domes in EN medium (A, scale = 1 mm and B, scale = 0.2 mm). Organoids were assessed by H&E staining (C, scale = 50 μm). Organoids were positive for KRT5 immunofluorescence (D, day 5, scale = 50 μm) at culture day 5. **(F)** Optimal organoid proliferation was observed at cells densities between 300-500 cells/μL BME at passage 0. **(G)** UABCs suspended in OPTI-MEM showed more INDELs compared to UABCs suspended in P2 solution indicating improved delivery of the Cas9/sgRNA complex. **(H)** Pre-treatment of UABCs for 48h with RI improved the survival and proliferation of edited UABCs. Error bars represent standard deviation in all panels.

Figure S2

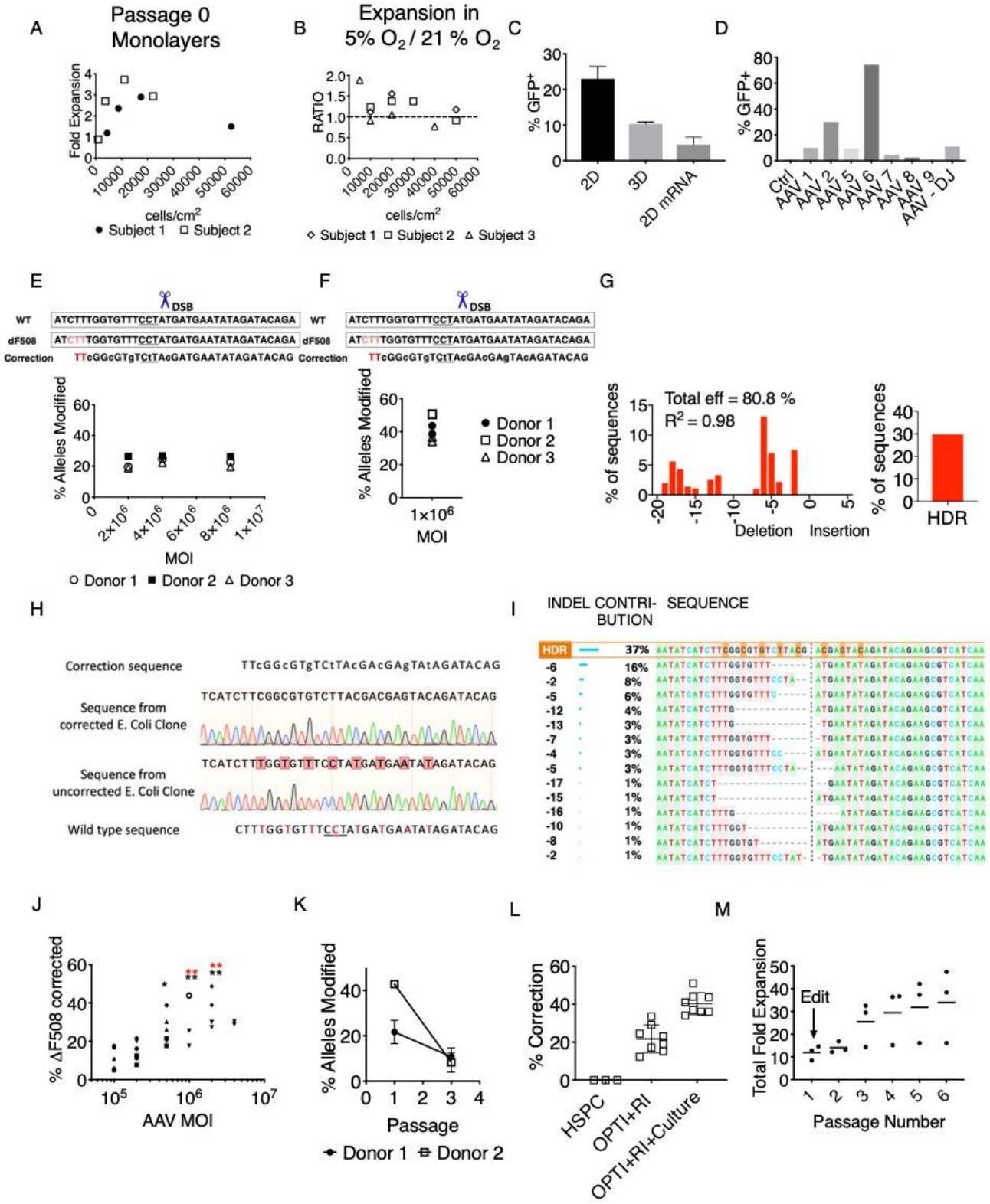
A
Passage 0 Monolayers
Fold Expansion
cells/cm2
Subject 1 Subject 2
B
Expansion in 5% O2 / 21 % O2
RATIO
cells/cm2
Subject 1 Subject 2 Subject 3
C
% GFP+
2D
3D
2D mRNA
D
% GFP+
Ctrl
AAV 1
AAV 2
AAV 5
AAV 6
AAV 7
AAV 8
AAV 9
AAV - DJ
E
DSB
WT ATCTTTGGTGTTTCCTATGATGAATATAGATACAGA
dF508 ATCTTTGGTGTTTCCTATGATGAATATAGATACAGA
Correction TTcGGcGTgTCtTAcGATGAATATAGATACAG
% Alleles Modified
MOI
Donor 1 Donor 2 Donor 3
F
DSB
WT ATCTTTGGTGTTTCCTATGATGAATATAGATACAGA
dF508 ATCTTTGGTGTTTCCTATGATGAATATAGATACAGA
Correction TTcGGcGTgTCtTAcGAcGAgTAcAGATACAG
% Alleles Modified
MOI
Donor 1
Donor 2
Donor 3
G
Total eff = 80.8 %
R2 = 0.98
% of sequences
Deletion Insertion
% of sequences
HDR
H
Correction sequence TTcGGcGTgTCtTAcGAcGAgTAtAGATACAG
Sequence from corrected E. Coli Clone TCATCTTCGGCGTGTCTTACGACGAGTACAGATACAG
Sequence from uncorrected E. Coli Clone TCATCTTTGGTGTTTCCTATGATGAATATAGATACAG
Wild type sequence CTTTGGTGTTTCCTATGATGAATATAGATACAG
I
INDEL CONTRI-BUTION
SEQUENCE
HDR 37%
-6 16%
-2 8%
-5 6%
-12 4%
-13 3%
-7 3%
-4 3%
-5 3%
-17 1%
-15 1%
-16 1%
-10 1%
-8 1%
-2 1%
J
% ΔF508 corrected
AAV MOI
K
% Alleles Modified
Passage
Donor 1 Donor 2
L
% Correction
HSPC
OPTI+RI
OPTI+RI+Culture
M
Total Fold Expansion
Edit
Passage Number

Figure S2. Improved gene editing in UABC monolayers versus 3D organoids, Related to Figure 1. (A) Primary human UABCs were cultured as monolayers in tissue culture treated plates coated with 5% BME in EN medium. Optimal UABC proliferation was observed at cells densities between 10,000-20,000 cells/cm^2 at passage 0. **(B)** Culturing UABC monolayers in 5% O_2 improved proliferation of cells from 2 out of 3 subjects (subjects 1 and 2). **(C)** Cells cultured both as monolayers and organoids were edited using Cas9 RNP to express SFFV/GFP at the CCR5 locus using a previously reported construct (Hendel et al., 2015). Editing efficiencies were higher for cells cultured as monolayers (N = 3, p = 0.02 by paired t-test). We also tested the use of Cas9 mRNA to edit UABCs but found the strategy to be less efficient. **(D)** AAV6 showed the best transduction in upper airway basal cells (UABCs). UABCs were transduced within 5 min after electroporation. **(E-F)** Two different correction templates with varying amounts of silent mutations (lower case letters) around the DSB site (scissors) were tested. PAM sequence is underlined. Templates with 8 silent mutations distributed on both sides of the DSB site (F) resulted in higher HR than templates containing 5 mutations on one side (E). **(G)** Example results from TIDER analysis of a corrected CF sample showing the distribution of INDELs and percent of sequences with the correction sequence. **(H)** A non-CF sample was edited. The PCR product used for TIDER was cloned into a TOPO plasmid and transformed into E. Coli (Dever et al., 2016). We screened 50 clones to verify the integration of the correction sequence. Example traces from an uncorrected clone and a corrected clone are shown. **(I)** The results from TIDER were also compared using another analysis tool named ICE developed by Synthego Inc. and we observed similar HR and INDEL levels using both analyses. The ICE result for the sample shown in (A) is presented here. **(J)** In UABCs obtained from non-CF patients, MOIs of 10_6 and $2x10_6$M vector genomes (vg)/cell showed significantly higher editing compared to MOIs < $2x10_5$ vg/cell (* $p < 0.05$, ** $p < 0.01$ with respect to $1x10_5$ (black) and $2x10_5$ (red)). Different symbols represent cells from a different donor**. (K)** The allelic insertion of the HR template decreased from 28 ± 12 % when UABCs were edited in passage 1 to 9 ± 4 % when UABCs were edited after passage 3. UABCs were therefore edited only in passage 1 for further experiments. **(L)** The use of OPTI-MEM and RI treatment enabled the insertion of the ΔF508 correction sequence in 22 ± 7% alleles. The editing protocol using passage 1 UABCs cultured in monolayers at the optimal cell density in 5% O_2 resulted in a further improvement of gene insertion to 41 ± 6% alleles. **(M)** UABCs edited in passage 1 recovered by passage2 and then expanded to result in a 25 ± 10-fold (mean ± standard deviation) expansion by passage 3 and 34 ± 16-fold expansion by passage 6. . Error bars represent standard deviation in all panels.

Figure S3

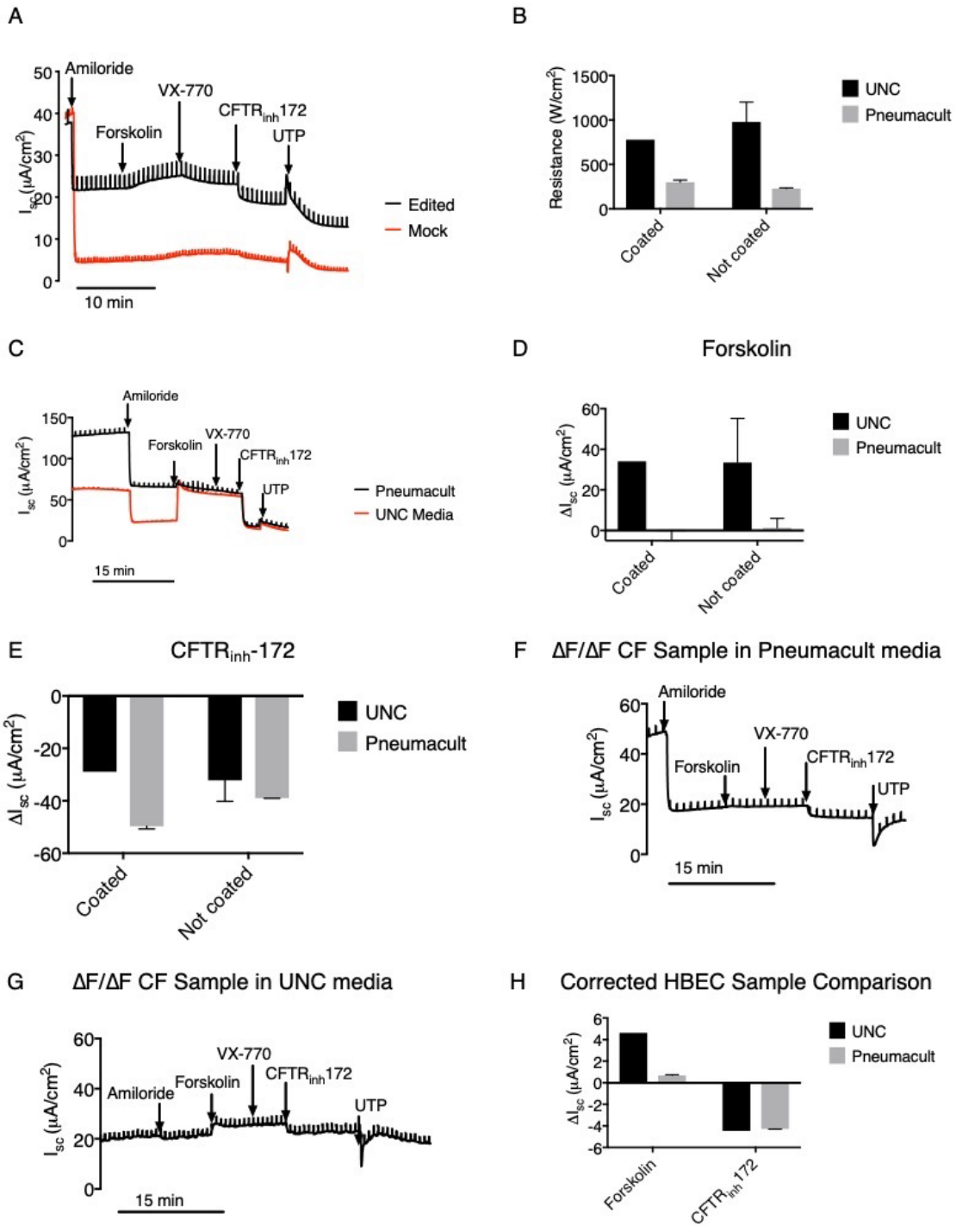
A
Amiloride
VX-770
CFTRinh172
Forskolin
UTP
Isc (μA/cm2)
Edited
Mock
10 min
B
Resistance (W/cm2)
UNC
Pneumacult
Coated
Not coated
C
Amiloride
Forskolin
VX-770
CFTRinh172
UTP
Isc (μA/cm2)
Pneumacult
UNC Media
15 min
D
Forskolin
ΔIsc (μA/cm2)
UNC
Pneumacult
Coated
Not coated
E
CFTRinh-172
ΔIsc (μA/cm2)
UNC
Pneumacult
Coated
Not coated
F
ΔF/ΔF CF Sample in Pneumacult media
Amiloride
VX-770
Forskolin
CFTRinh172
UTP
Isc (μA/cm2)
15 min
G
ΔF/ΔF CF Sample in UNC media
VX-770
Amiloride
Forskolin
CFTRinh172
UTP
Isc (μA/cm2)
15 min
H
Corrected HBEC Sample Comparison
ΔIsc (μA/cm2)
UNC
Pneumacult
Forskolin
CFTRinh172

Figure S3: Characterization of CFTR function, Related to Figure 2 and Table 1. (A) Representative traces obtained from epithelial monolayers derived from ΔF508 homozygous (ΔF/ΔF) CF HBECs (Mock). Correction of ΔF508 mutation in 30% of alleles resulted in a restoration of CFTR function. **(B)** UABCs from non-CF patients cultured in UNC media showed higher transepithelial resistances after differentiation in ALI **(C)** Representative traces from epithelial monolayers cultured in Pneumacult™ ALI and UNC media. Monolayers cultured in UNC media showed a more pronounced forskolin response. **(D)** In non-CF samples, short-circuit currents in response to forskolin were higher in monolayers cultured in UNC media. The presence or absence of collagen IV coating did not affect forskolin responses **(E)** Responses to $CFTR_{inh}$-172 were similar between monolayers cultured in UNC media and Pneumacult ALI™ for non-CF cells. The presence or absence of collagen IV coating did not affect $CFTR_{inh}$-172 responses **(F)** Upper airway basal cells from ΔF508 homozygous patient were edited (27% allelic correction) and differentiated using Pneumacult ALI™ and **(G)** UNC media (no collagen IV coating) on ALI membranes. **(H)** Similar to non-CF UABCs (C-D), responses to $CFTR_{inh}$-172 were similar between monolayers cultured in UNC media and Pneumacult™ ALI but monolayers cultured in UNC media showed higher forskolin-stimulated short-circuit currents. Error bars represent standard deviation in all panels.

Figure S4

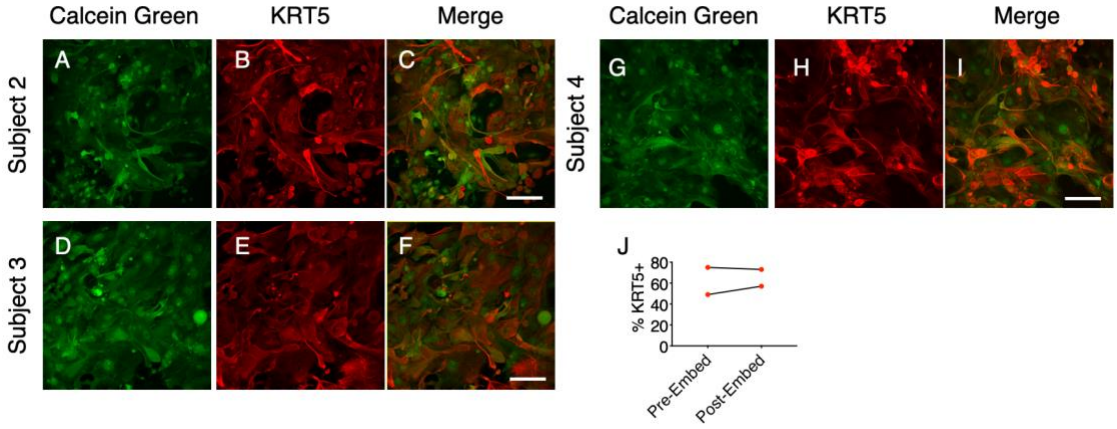

Figure S4: Embedding edited UABCs on pSIS membrane, Related to Figure 3. (A-I) Sheets fixed on day 4 after embedding on pSIS membrane were KRT5+. Calcein green indicates live cells and KRT5+ UABCs are stained red. Images from 3 additional subjects are shown here (scale = 100 μm). **(J)** The fraction of KRT5+ cells was measured by flow cytometry on the day of embedding onto pSIS membranes (Pre-embed). The fraction of calcein green positive cells that were also KRT5+ 4 days after embedding was determined using confocal microscopy (Post-embed). The fraction of KRT5+ cells were similar indicating that edited cells did not experience a proliferative disadvantage. These data suggest that the pSIS membrane is a suitable scaffold to optimize transplantation of corrected cells in animal models

Table S1: Off-target Activity of MS-SgRNA, Related to Figure 1. Cas9 can induce double stranded breaks even if there are a few mismatches exist between the target genomic DNA and sgRNA. As a result, undesired insertions and deletions at off-target (OT) sites may occur. The MS-sgRNA targeting the ΔF508 locus shows very low levels of OT activity (< 0.2%) at one locus (OT-41) and high levels of on-target activity. Mismatches are highlighted in bold and the protospacer adjacent motif (PAM) is underlined.

	Protospacer - PAM	Mock	Edited Subject 1	Edited Subject 1	Edited Subject 2	Gene
On target	TCTGTATCTATATTCATCATAGG	0.00	73.63	80.87	77.12	CFTR
OT1	T**T**TA**G**TCTATATTCATCATGGG	0.01	0.00	0.00	0.00	SLC4A10
OT2	**CA**TT**T**TATTCATCATGGG	0.00	0.00	0.00	0.00	TTTY5
OT3	**CA**TT**T**TATTCATCATGGG	0.00	0.00	0.00	0.02	TTTY12
OT4	**A**CT**TG**AT**T**TATATTCATCATAGG	0.00	0.00	0.00	0.00	MBL2
OT5	**A**C**A**GTAT**AA**ATATTCATCATAGG	0.00	0.00	0.00	0.00	PPIA
OT6	**C**CT**T**TAT**AC**ATATTCATCATTGG	0.00	0.00	0.01	0.01	NLRP2B
OT7	**AT**TGT**T**TCT**C**TATTCATCATTGG	0.01	0.01	0.00	0.00	FAM169A
OT8	**A**CTGTA**AAC**ATATTCATCATAGG	0.00	0.00	0.00	0	PHF21B
OT9	**G**CTG**C**ATC**AT**TATTCATCATCGG	0.01	0.00	0.01	0.00	OR6K6
OT10	**TT**TG**C**ATCTAT**G**TTCATCATAGG	0.01	0.00	0.01	0.01	UBA6-AS1
OT11	**TT**TG**C**ATCTAT**G**TTCATCATGGG	0.00	0.00	0.00	0	RGMB
OT12	**TT**TGT**G**TCTAT**G**TTCATCATAGG	0.00	0.00	0.01	0.00	MOCOS
OT13	**TT**TGT**G**TCTAT**G**TTCATCATGGG	0.00	0.00	0.00	0.00	RANBP17
OT14	**A**CTGT**G**TC**C**A**G**ATTCATCATAGG	0.00	0.00	0.00	0.00	COL11A1
OT15	**A**CTGTA**G**C**A**A**A**ATTCATCATTGG	0.00	0.00	0.00	0.00	VIM-AS1
OT16	**T**CT**A**TATCT**TC**ATTCATCATGGG	0.00	0.01	0.09	0.00	LRRTM4
OT17	**C**CT**A**T**C**TCTATA**A**TCATCATGGG	0.00	0.01	0.01	0.00	MTHFS
OT18	TCTG**C**ATCTATAT**A**CATCATCAG	0.00	0.01	0.01	0.00	MSS51
OT19	TCT**T**T**C**TCTATAT**C**CATCATAGG	0.01	0.00	0.00	0.01	MIR4451
OT20	TCTGT**T**T**A**TATAT**C**CATCATGGG	0.01	0.01	0.01	0.00	NCAM2
OT21	**A**CTGTA**A**CTAT**TC**TCATCATAGG	0.00	0.00	0.00	0.00	RNF141
OT22	**GG**T**C**TATCTATATT**T**ATCATTGG	0.01	0.01	0.01	0.02	NRG1
OT23	**A**CTGTATC**A**ATATT**G**ATCATTAG	0.02	0.03	0.01	0.01	MIR488
OT24	**C**CT**A**TATCTAT**C**T**A**CATCATAGG	0.01	0.00	0.00	0	XIRP2
OT25	TCT**A**TAT**T**TATATT**A**ATCATAGG	0.02	0.02	0.01	0	LINC01243
OT26	**C**CTGT**G**TCTAT**G**TT**T**ATCATAGG	0.01	0.00	0.00	0.03	LOC105374194
OT27	**C**CT**T**TATCTATATTCA**C**CATGGG	0.00	0.01	0.00	0.00	CALM2
OT28	**A**CTG**C**ATCTAT**G**TTC**T**TCATGGG	0.00	0.00	0.01	0.00	OTOR
OT29	**C**CT**A**TATC**C**ATATTCA**C**CATTGG	0.02	0.02	0.01	0.01	NRP2
OT30	TCTGT**G**TCTATA**A**TC**T**TCATAGG	0.00	0.02	0.02	0.01	MGAT4C

OT31	**G**CT**A**TATCTATAT**C**C**T**TCATTGG	0.02	0.04	0.01	0.00	LOC101927394
OT32	**C**CTGTAT**A**TATATTCAT**A**ATTAG	0.01	0.02	0.01	0.02	LOC100422212
OT33	TCTGTAT**G**TATATTCAT**G**ATGAG	0.00	0.00	0.01	0.00	PSD3
OT34	TCT**A**TATCTATA**G**TCA**G**CATTGG	0.00	0.00	0.00	0.00	MRGPRX3
OT35	**C**CTGTATCTAT**T**TTCAT**A**ATGAG	0.018	0.022	0.06	0.016	MACROD2
OT36	**C**CTGTATCTATATT**A**A**A**CATAGG	0.02	0.01	0.00	0.01	MIR5011
OT37	TCTGTATCTATATTCATCA-GGG	0.00	0.01	0.01	0.01	CNTNAP5
OT38	TCTGTATCTAT**G**TTCATCA**C**AGG	0.00	0.01	0.01	0.00	LINC00331
OT39	**A**CTGTATCTATATTCAT**A**A**G**GGG	0.02	0.02	0.01	0.03	LOC101928437
OT40	T**T**TGT**G**TCTATATTCAT**A**ATAGG	0.02	0.01	0.01	0.00	LOC102723895
OT41	**TCTATATCTATATACACCATAGG**	**0.01**	**0.18**	**0.15**	**0.224**	**DIXDC1**
OT42	**G**CTGTAT**T**TATAT**C**CA**A**CATGGG	0.00	0.00	0.00	0	LINC00618
OT43	**G**CTGTATCT**T**TA**C**TCA**C**CATTGG	0	0	0	0	VCX3B
OT44	TCTG**C**AT**G**TATATTCATCA**G**TGG	0.00	0.00	0.01	0.01	MRGPRX3
OT45	**G**CTG**A**ATCTATATT**G**ATC**C**TGGG	0.01	0.00	0.00	0.00	DNAH6
OT46	**A**CTGT**T**TCTATATT**T**ATC**G**TAGG	0.03	0.01	0.00	0.07	GARNL3
OT47	TCTGTAT**T**TATATT**T**ATC**C**TGGG	0.01	0.01	0.01	0.01	ATP6V0D2